ICAS Paper No. 70–55

THE EFFECT OF LATERAL CONTROL NON-LINEARITIES ON THE HANDLING QUALITIES OF LIGHT STOL AIRCRAFT A FLIGHT SIMULATOR STUDY

by
D. R. Madill, O.M.S. Colavincenzo, Aerodynamicists
de Havilland Aircraft of Canada, Ltd.
and
W. E. B. Roderick, Research Engineer
National Aeronautical Establishment, Canada

The Seventh Congress of the International Council of the Aeronautical Sciences

CONSIGLIO NAZIONALE DELLE RICERCHE, ROMA, ITALY / SEPTEMBER 14-18, 1970

Price: 400 Lire

THE EFFECTS OF LATERAL CONTROL NON-LINEARITIES ON THE HANDLING QUALITIES OF LIGHT STOL AIRCRAFT - A FLIGHT SIMULATOR STUDY*

D. R. Madill and O. M. S. Colavincenzo,
Aerodynamicists,

The de Havilland Aircraft of Canada, Limited, Downsview, Ontario

and

W. E. B. Roderick,
Research Engineer,

National Research Council of Canada

*This research was sponsored in part by
The Defence Research Board of Canada
under Grant No. DRB 0301-20

ABSTRACT

The effects of wheel force and roll moment non-linearities on the handling qualities of light STOL aircraft on approach are examined, using the NAE variable stability helicopter. Emphasis is on manual control but a few powered control results are also presented. Pilot opinion ratings and questionnaire replies form the data basis for this study. Statistical techniques are used to remove pilot bias in the rating data and to improve the sensitivity of the experiment. The projection of the results to larger STOL aircraft is considered briefly.

I INTRODUCTION

The tremendous air-traffic potential for short to medium-range operations has resulted in a recent intensive development of STOL aircraft. This has been manifest in a quest for lower approach speeds, shorter landing and takeoff runs, and larger payload capabilities through the development of powered-lift techniques, more effective flap systems and ever increasing flap spans.

Unfortunately, the same factors which contribute to improved STOL performance detract from the lateral handling qualities. In particular, aileron spans diminish with increasing flap spans while the effects of slipstream lift place an increasing demand on aircraft roll control power. As a consequence, attention has turned progressively toward spoilers for lateral control.

However, spoilers have their own particular problems. Not the least of these is the fact that spoiler characteristics are generally non-linear functions of aircraft configuration, flap setting and spoiler deflection. Clever mechanical design can alleviate some of the non-linear response characteristics but mechanical inversion of all non-linearities is extremely difficult, and more sophisticated electro-hydraulic solutions to the problem are hard to justify in light aircraft. The residual non-linearities, on the other hand, can detract from the aircraft handling qualities and render precision manoeuvres and fine control beyond the capability of most pilots. In some cases the result may be overcontrol or pilot induced oscillation,

This paper outlines a study undertaken to examine non-linear effects on lateral handling qualities as influenced by several basic aircraft and control system parameters including control friction, adverse yaw, and turbulence. The non-linearities were introduced in the lateral control forces and lateral aerodynamic response only. The remainder of the aircraft characteristics were linear. The basic simulation centered on a small STOL transport of 7000 lb. gross weight. However, some results for a medium STOL aircraft of 37,000 lb. gross weight are included.

While fixed-base installations can adequately simulate basic aerodynamic characteristics for some pilot tasks, the dynamic and kinesthetic environment are often as important as aerodynamic characteristics in the evaluation of aircraft handling qualities. In recognition of the importance of the total dynamic environment, this study was carried out in an airborne simulator. Evaluation was performed while executing a critical but realistic STOL approach task.

II SIMULATOR

The vehicle for the airborne simulation was a variable stability Bell 47G-3B1 helicopter (Figure 1) operated by the Flight Research Section of the National Aeronautical Establishment (1). This is a four-degrees-of-freedom simulator using the model-control method (2). The required equations of motion are programmed on an analogue computer. The evaluation pilot control inputs drive the analogue model, and the calculated angular rates are matched by the helicopter autopilot.

The simulator has independent control of pitch, roll, yaw, and heave; but since there is no independent means of generating longitudinal or lateral forces, the characteristics in these two translational degrees-of-freedom are essentially those of the helicopter, modified somewhat by the rotational simulation. Despite these limitations the helicopter has proven to be an effective lateral-directional simulator for STOL aircraft (3).

Non-linear wheel force characteristics for the evaluation pilot were simulated via a servo-actuator

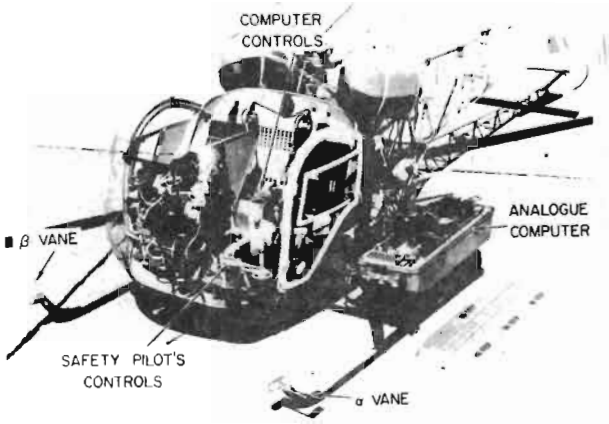

NAE FLIGHT SIMULATOR

FIGURE 1

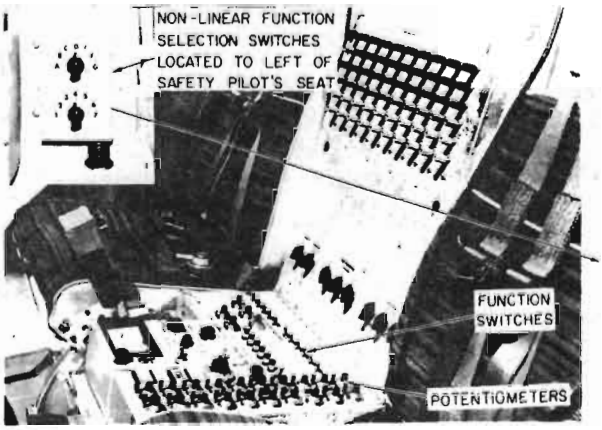

COCKPIT CONTROLS LEFT HAND SEAT

FIGURE 3

system installed on the wheel in the right-hand cockpit (Figure 2). Longitudinal and directional control forces, supplied by mechanical springs, had linear gradients that were not varied during the program. The safety pilot, acting as airborne program manager, could alter the simulator characteristics at will, by means of the computer controls and function switches in the left-hand cockpit (Figure 3).

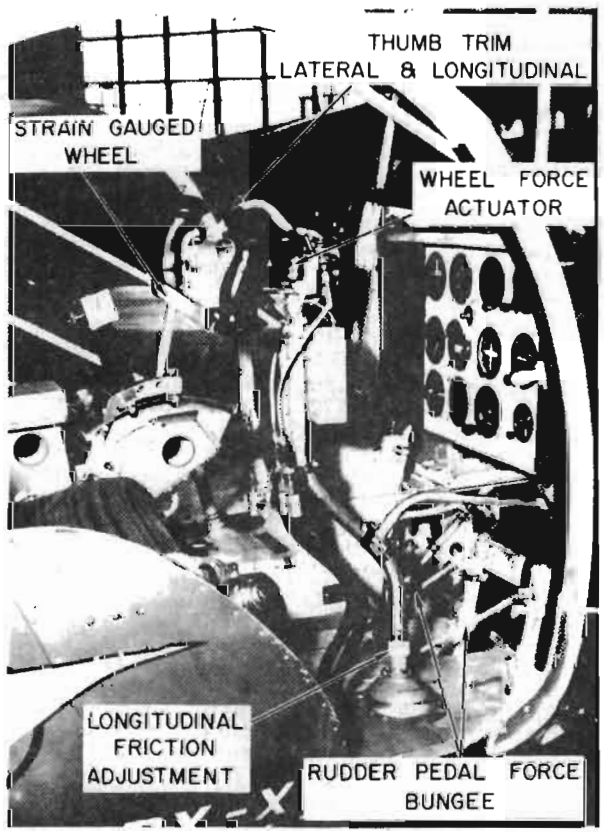

COCKPIT ANALOGUE CONTROLS RIGHT HAND SEAT

FIGURE 2

The lateral control system for the evaluation pilot included provision for simulation of friction (hysteresis) and control dynamics (inertia) and damping) in addition to the non-linear wheel force characteristics (Figure 4). The system also produced the non-linear aerodynamic characteristics for the aircraft simulation. The simulated aileron was directly driven by wheel position. The spoiler could be directly coupled to the aileron or powered with non-linear actuator valve characteristics and valve force feedback.

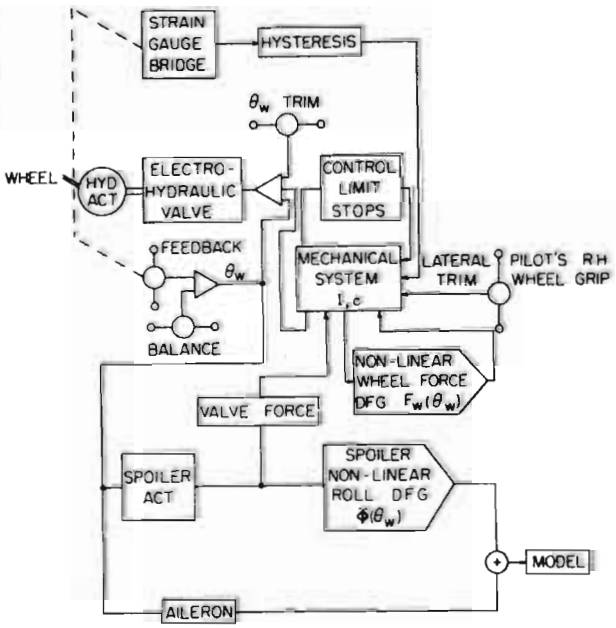

NON-LINEAR FEEL SYSTEM BLOCK DIAGRAM

FIGURE 4

Fixed-diode-function generators were used in both the lateral aerodynamic and wheel force simulations for accurate, repeatable, rapid selection of the desired non-linear characteristics.

Synthetic turbulence was injected directly into the analogue simulation in the pitch and yaw channels but not in the heave channel. The RMS gust levels were set at σ_W = 2 fps and σ_V = 3 fps respectively for the basic simulation but provision was made for adjusting these levels. External side gusts were sensed through helicopter roll and yaw accelerations and resisted by the autopilot. No attempt was made to arrest the corresponding helicopter vertical gust response. However, because of the inherently low pitch response of the helicopter to vertical gusts and since the evaluation was only carried out under relatively calm and stable atmospheric conditions, it was felt that external pitch disturbances were negligible.

An approximation to the von Kármán spectrum was used for the gust intensity distribution with scale lengths for L_V and L_W of 1000 and 200 feet respectively.

Crosswinds could be introduced in the simulator by biasing the helicopter β vane. This meant that the crosswind followed helicopter yaw excursions and was not entirely realistic. However, the differences between this and a true simulation were considered small for the approach segment of the task. External crosswinds were eliminated by positioning of the glide slope and runway markers.

III TASK

The evaluation of each configuration was carried out in four consecutive segments, combined to form a VFR circuit and approach task (Figure 5). The first segment, the downwind and crosswind portion of the circuit, was used to establish the characteristics of the model. The pilot was instructed to perform rolling and yawing manoeuvres to familiarize himself with the aircraft response.

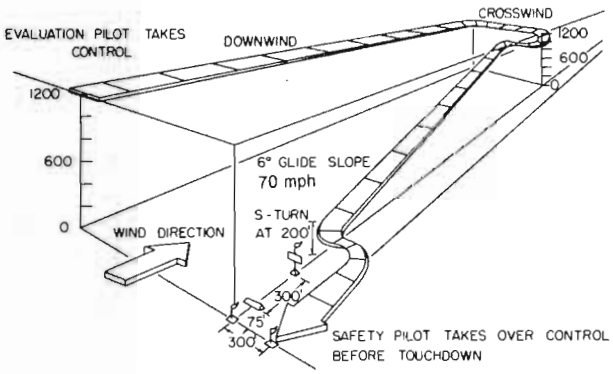

VISUAL FLIGHT TASK FOR STOL LATERAL - DIRECTIONAL HANDLING QUALITIES EVALUATION

FIGURE 5

The crosswind leg terminated after glide path interception with a sharp 90° turn, performed as rapidly as possible consistent with normal safety requirements, on to the simulated approach path. This manoeuvre, requiring gross control movements and a measure of precise control for rapid accurate acquisition of the approach glide slope, formed the second segment of the task.

The third segment, accurate tracking down a 6° glide slope, was performed with several restrictions on pilot technique. The aircraft was not to be crabbed into the simulated crosswinds but was to be sideslipped, requiring lateral control offset and cross control during the approach. Also, aileron and rudder trim were not to be used during this portion of the task.

The final segment of the evaluation was a rapid three-hundred foot sidestep manoeuvre, initiated at an altitude of two-hundred feet above ground, followed by a simulated landing.

Prior to the actual evaluation program, each of the four participating pilots was given a one-hour familiarization flight in the simulator. All the parameters to be studied were demonstrated but particular configurations were not identified. A ground briefing outlined the purpose of the project, the parameters to be varied, the method of evaluation and the task. Dialogue between the evaluation pilots and project engineers was encouraged and the nature of the exercise, as an aircraft handling evaluation and not an aircrew skill test, was emphasized. The importance of confident, objective, experienced and motivated personnel in a project of this kind cannot be overstressed.

A modified Cooper Rating scale was used (Figure 6) and at the completion of each configura-

CONTROLLABLE capable of being controlled or managed in context of mission, with available pilot attention	ACCEPTABLE May have deficiencies which warrant improvement but adequate for mission. Pilot compensation if required to achieve acceptable performance is feasible.	SATISFACTORY Meets all requirements and expectations. Good enough without improvement. Clearly adequate for mission.	Excellent. Highly desirable	A1
			Good. Pleasant. Well behaved	A2
			Fair. Some mildly unpleasant characteristics. Good enough for mission without improvement.	A3
		UNSATISFACTORY Reluctantly acceptable. Deficiencies which warrant improvement. Performance adequate for mission with feasible pilot compensation.	Some minor but annoying deficiencies. Improvement requested. Effect on performance easily compensated for by pilot.	A4
			Moderately objectionable deficiencies. Improvement needed. Reasonable performance requires considerable pilot compensation.	A5
			Very objectionable deficiencies. Major improvements needed. Requires best available pilot compensation to achieve acceptable performance.	A6
	UNACCEPTABLE Deficiencies which require mandatory improvement. Inadequate performance for mission even with maximum feasible pilot compensation.		Major deficiencies requiring mandatory improvement for acceptance. Controllable. Performance inadequate for mission or pilot compensation required for minimum acceptable performance in mission is too high.	U7
			Controllable with difficulty. Requires substantial pilot skill and attention to retain control and continue mission.	U8
			Marginally controllable in mission. Requires maximum available pilot skill and attention to retain control.	U9
UNCONTROLLABLE Control will be lost during some portion of mission.			Uncontrollable in mission	10

PILOT OPINION RATING SYSTEM

FIGURE 6

tion evaluation, a questionnaire was filled in by the pilot (Figure 7). The purpose of this was to help correlate pilot comments and, if possible, establish the basis for pilot rating. During the program the various configurations were presented to the evaluation pilot in a random fashion without prior identification.

CONFIGURATION _____

PILOT _____

DATE _____

PILOT RATING

Overall assessment of Lateral Control Qualities _____

DEFICIENCIES REFLECTED IN PILOT RATING

a) Symmetric Control Characteristics

1. Wheel force for small displacements — too high ☐ low ☐
2. Wheel force for large displacements — too high ☐ low ☐
3. Roll power for small displacements — too high ☐ low ☐
4. Roll power for large displacements — too high ☐ low ☐
5. Wheel centering tendency inadequate ☐
6. Aileron rate-limiting objectionable ☐
7. Lag in roll response objectionable ☐

b) Asymmetric Control Characteristics

8. Differential wheel force effects objectionable ☐
9. Differential roll power effects objectionable ☐
10. Wheel travel to hold "sideslip" too high ☐
11. Wheel force to hold "sideslip" too high ☐
12. Rudder travel to hold "sideslip" too high ☐
13. Rudder force to hold "sideslip" too high ☐

c) Other Control and Aircraft Characteristics

14. Pilot induced oscillation tendencies objectionable ☐
15. Aileron adverse yaw objectionable ☐
16. Turn co-ordination difficult ☐
17. Control harmony poor ☐
18. Gust sensitivity — too high in roll ☐ yaw ☐
19. Lateral stability — too high ☐ low ☐
20. Directional stability — too high ☐ low ☐

QUESTIONNAIRE

FIGURE 7

IV TEST CONFIGURATIONS

Basic Small STOL Aircraft

The basic aircraft simulated in this study was a small STOL aircraft, weighing 7000 lb. (Table 1). It was equipped with a manual control system (aileron and spoiler directly coupled) which had inertia, damping and non-linear static force elements but no friction, preload or aerodynamic force feedback (Table 2). The control system damping, which was high for small wheel velocities and low for high velocities, was required for control system stability in the simulator and was, on the average, higher than is generally found in lateral control systems. The simulated non-linear wheel forces are given in Figure 8, and were composed of two essentially straight line segments with a maximum force of 20 lb.

The roll acceleration characteristics are given in Figure 9, and were selected from the phase angle characteristics of a second-order system normalized at twice the undamped natural frequency. These roll acceleration curves cover the spectrum of non-linearities observed in practice for a variety of spoiler types. The maximum roll acceleration was 2.42 rad/sec.^{2}.

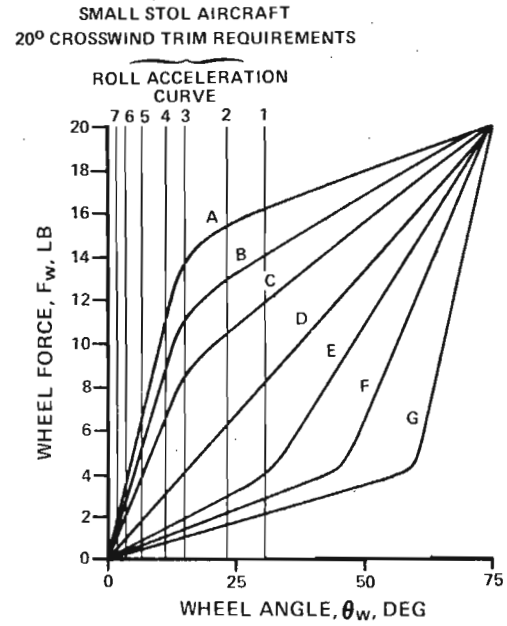

SIMULATED NON-LINEAR WHEEL FORCES

FIGURE 8

For purposes of subsequent identification, the non-linear wheel force and roll acceleration characteristics are assigned the letters A - G and numerals 1 - 7 respectively.

In addition to this basic aircraft configuration, eight configurations or "blocks" representing variations in the aircraft geometry, flight environment

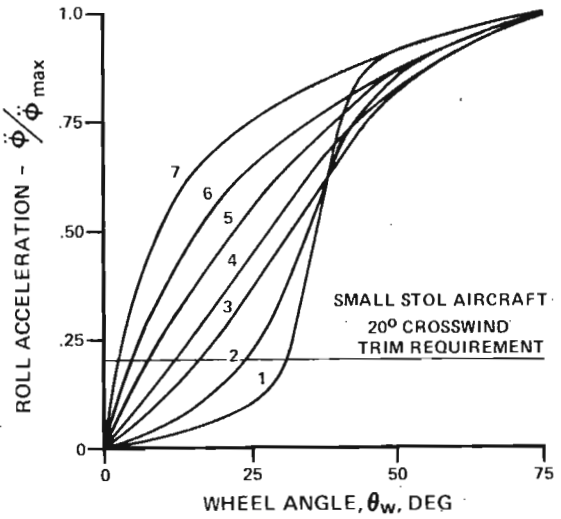

SIMULATED NON-LINEAR ROLL ACCELERATIONS

FIGURE 9

and control system characteristics were simulated. These are described below:

Basic + Gust. In this block the basic RMS turbulence levels of σ_W = 2 and σ_V = 3 fps were increased to 4 and 6 fps respectively.

Basic + Crosswind. A crosswind was introduced for the tracking and sidestep segments of the task by biasing the β vane 20° in 1.0 sec. at the start of the tracking segment. Because the pilot was constrained to sideslip the aircraft on approach, this crosswind could result in large wheel "trim" angles and control asymmetries, depending on the non-linear roll acceleration characteristics. These effects are evident from Figures 8 and 9 where the 20° crosswind "trim" requirements are noted.

Basic + Friction. The basic wheel force characteristics of Figure 8 were modified by adding a 5 lb. friction force at the wheel. Hysteresis was used to represent the control friction. This is a simplified representation but was considered adequate for this study.

Basic + $C_{n_{\delta A}}$. The aileron adverse yaw of the basic aircraft configuration was essentially zero. For the adverse yaw block, the maximum yawing acceleration due to aileron was set at 0.1 $\ddot{\Phi}$ max and was linear with control wheel deflection.

Basic + Dihedral. The effective wing dihedral on the basic aircraft was doubled by increasing the derivative C_{ℓ_β}.

Basic + Fin Change. The fin and rudder area on the basic aircraft were doubled by suitably modifying the appropriate roll, yaw and control derivatives. No changes were made in the rudder pedal forces.

Powered-Manual Control. For the powered-manual control block, the spoilers were powered while the ailerons were manually driven. The control system dynamics were the same as in the basic block but the static wheel force characteristic was linear (Figure 8, curve D).

The aileron roll acceleration was linear with wheel deflection and supplied 25% of the maximum acceleration at full deflection. The spoiler roll acceleration characteristics were those of Figure 9 less the linear aileron contribution.

The spoiler actuator had a manually operated valve with a series preload spring, a fixed valve stroke with no valve overrun, and a variable flow gain. The latter was defined by $^1/_T$, the inverse of the actuator time constant, and values of $^1/_T$ between 10 and 60 sec.$^{-1}$ were examined. For purposes of subsequent identification these $^1/_T$ values, which replace the wheel force non-linearities in the manual control studies, have been assigned the letters A - G respectively.

The valve flow characteristics, and the wheel forces arising from compression of the preload spring, are shown in Figure 10. The spring, which has an unlimited compression stroke, provides overrun when the pilot encounters the valve stops. The dynamic response of the spoiler actuator to a step valve input is shown in Figure 11.

Fully-Powered Control. For the fully-powered block, the spoilers were powered and supplied all of the available roll acceleration (2.42 rad/sec.^{2}). The control system dynamics were eliminated in this simulation. The static wheel force characteristic was linear (curve D of Figure 8) and the roll acceleration characteristics of Figure 9 were used.

The spoiler actuator had an electrically driven valve (Figure 10) and consequently did not supply

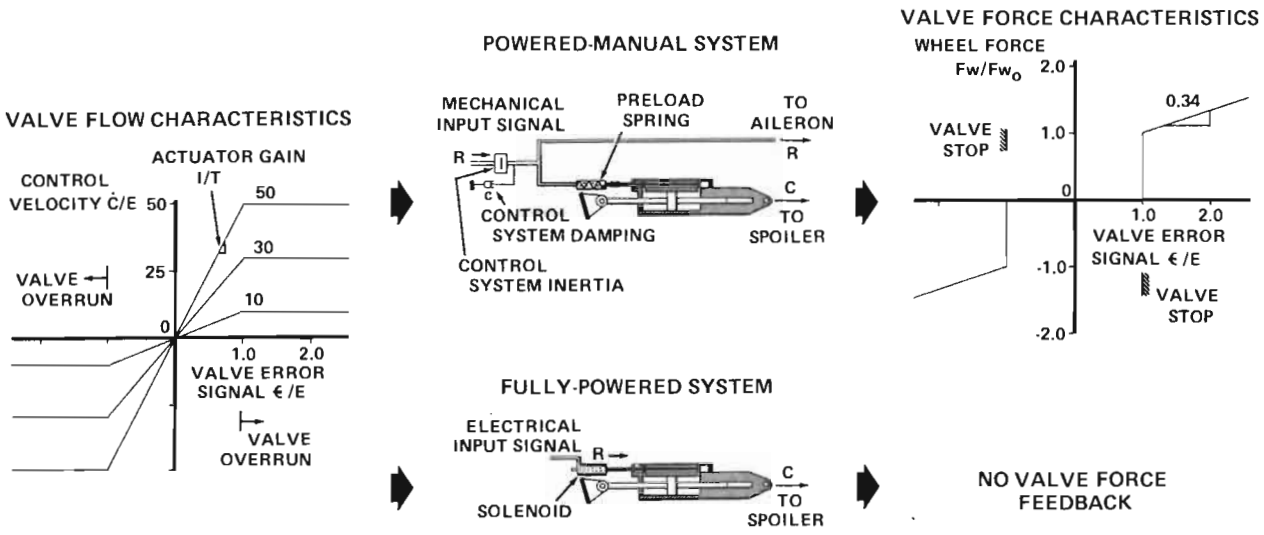

SIMULATED SPOILER ACTUATOR CHARACTERISTICS

FIGURE 10

force feedback. The valve flow gain $1/T$ was varied from 10 - 60 sec.$^{-1}$.

Basic Medium STOL Aircraft

The medium STOL aircraft results were obtained in a subsequent study using the same simulator, pilots and task. The aircraft weighed 37,000 lb., and was equipped with a manual control system similar to that on the small aircraft. A description of the aircraft and control system characteristics is given in Tables 1 and 2 respectively. The non-linear wheel forces and roll accelerations were those given in Figures 8 and 9 with $F_{w\,max}$ = 20 lb. and $\ddot{\Phi}$ max = 0.826 rad/sec.^{2}. The turbulence levels were set as before at σ_W = 2 and σ_V = 3 fps.

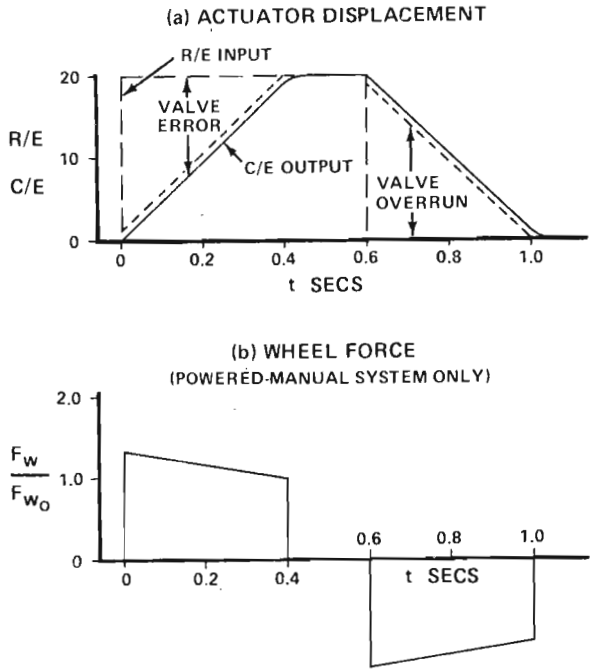

SPOILER ACTUATOR RESPONSE TO STEP VALVE COMMAND

FIGURE 11

Since the object of this study was to yield basic design information, the small aircraft blocks reflected perturbations in aircraft geometry that were consistent with design expectations. No attempt was made to perform a generalized transfer function study.

The simulation accuracy of the "basic" small and medium STOL aircraft configurations was verified against the performance of actual (and similar) STOL aircraft executing precisely the same task.

As a result of these trials the longitudinal simulation, which suffered from lack of helicopter thrust capability, was set at a nominal and comfortable level for the ensuing evaluations. Despite the absence of a helicopter side force capability, the lateral simulation was considered to be quite good. Evidence of a time delay of about 0.1 sec. in the helicopter roll control loop was obtained from earlier simulation efforts[3], and attributed to lag in tilting the rotor. However, this value is representative of typical aircraft spoiler lags and as such did not detract from the simulation.

V EXPERIMENTAL DESIGN

It was clearly impossible to have several pilots evaluate all combinations of the primary (non-linear wheel force, roll acceleration and actuator gain) parameters in each of the foregoing blocks; yet the variation in handling qualities with these parameters and the differences between pilots, constituted essential elements of the study.

This problem was circumvented through appropriate choice of the experimental design. The solution consisted of the statistical and response surface designs of Figure 12. In these designs, four pilots evaluated 12 primary parameter combinations ("configurations") in such a way that only two of the four pilots participated in the evaluation of any one configuration.

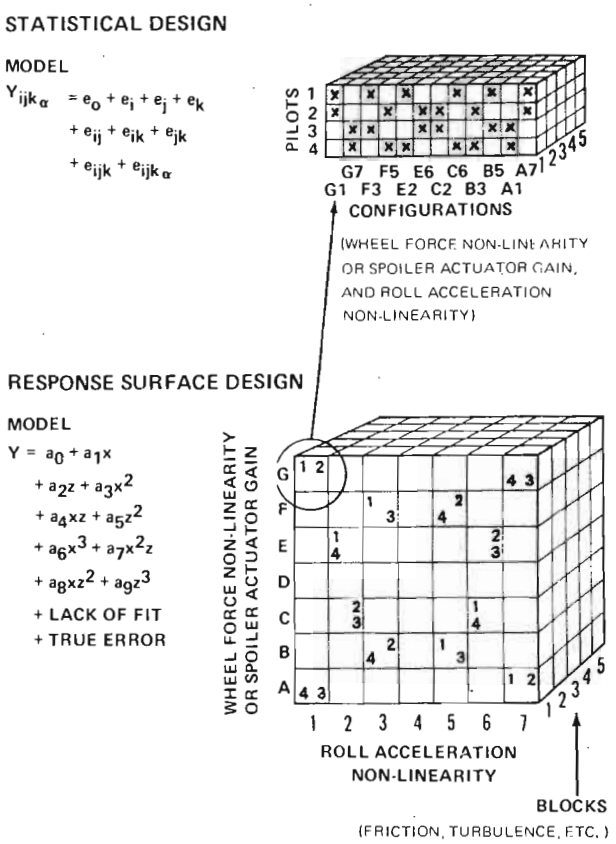

BASIC EXPERIMENTAL DESIGNS

FIGURE 12

Balanced designs were used to simplify the analysis and ensure a high level of precision [4]. The statistical design was balanced in the sense

that all pilots participated equally in the experiment and all pairs of pilots appeared the same number of times in the assessment of configurations (i.e. balanced-incomplete-block design). The response surface design was balanced such that all pilots participated in the assessment of each wheel force, actuator gain or roll acceleration non-linearity.

Pilots were assigned at random to the test configurations within these design constraints and the same experimental designs were used in the assessment of all "block" parameters.

While the experimental designs, so defined, constituted the basis of all experimental investigations reported here, some deviations from this design were of course inevitable. The available test time ultimately allowed some test points to be replicated, providing a measure of true error, and the "basic" blocks to be completed as full factorial designs (in the sense that all four pilots evaluated all 12 configurations).

VI PILOTS

Of the four pilots participating in the program, two were de Havilland, Canada test pilots with considerable STOL experience but very limited experience on flight simulators. The remaining two were NAE pilot-engineers whose recent flying experience had been related to handling qualities research on the flight simulator used in this study or some variant of this simulator. The flight experience of these four pilots is detailed in Table 3.

VII RESULTS AND ANALYSIS

The pilot rating results from this study are given in Figure 13. Repeated points are designated with an asterisk and the location of the rating within each grid element reflects the pilot who performed the evaluation. Thus a typical element takes the form:

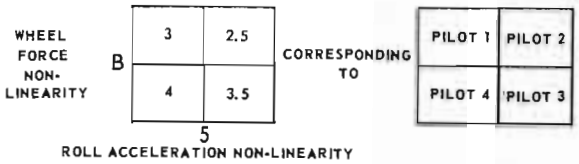

Ratings are presented for all the basic experimental designs with the exception of a few points that were rejected as a results of set-up errors. A few extra test points are also shown for some

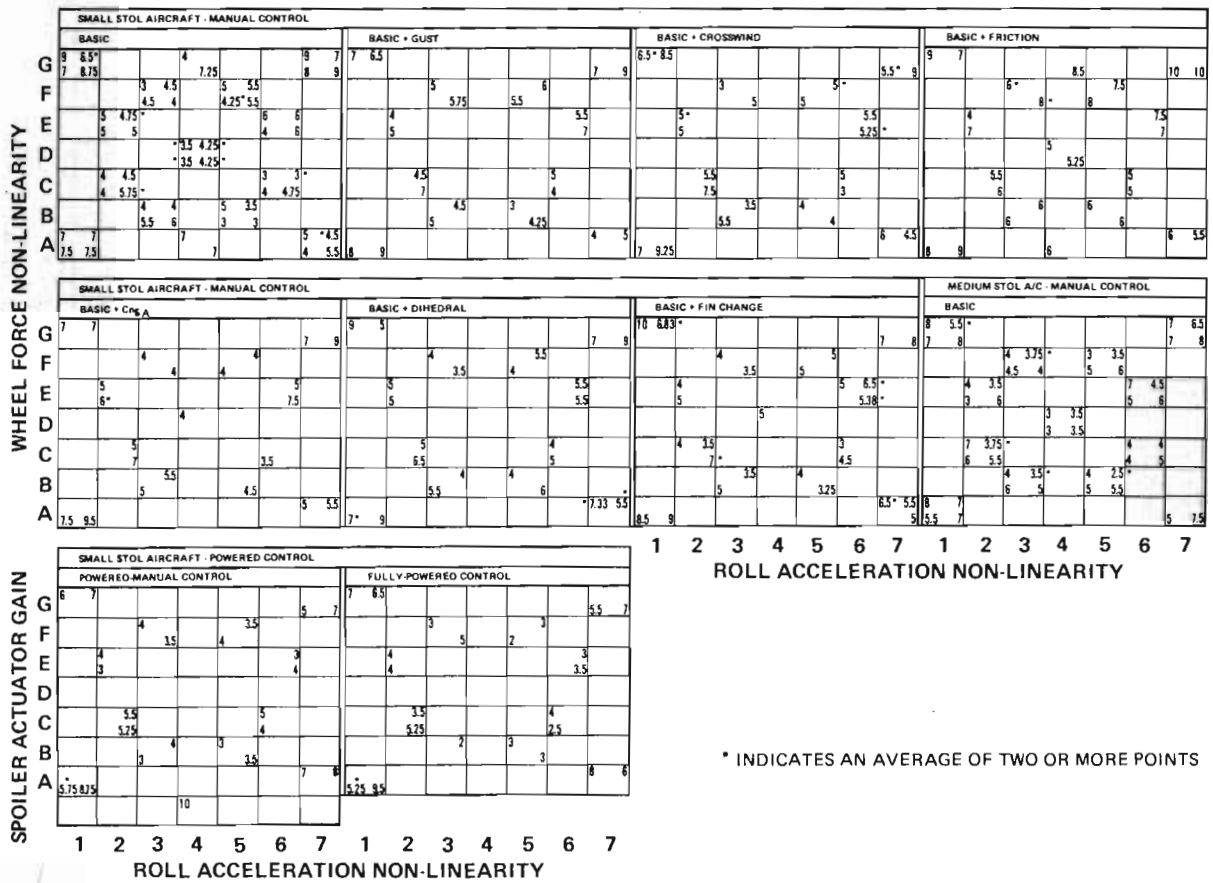

* INDICATES AN AVERAGE OF TWO OR MORE POINTS

PILOT RATINGS

FIGURE 13

of the blocks and these were, insofar as it was possible, incorporated in the analysis which follows. One of these extra points, however, required special consideration. This is the rating of 10 attributed to pilot 1 at the bottom of the small aircraft powered-manual control block. The actuator gain in this instance (not labelled) was $1/T = 5$. This point had been regarded as suspect in preliminary studies and as a result was disregarded in much of the subsequent analysis. Actually, for the most part, it will have a negligible effect on the results. It is introduced in the response surface analysis for the powered cases, however, because it critically affects the variation in rating with actuator gain.

Statistical Analysis of Pilot Ratings

Conventional analysis of variance techniques provide a means for detecting pilot bias and enable significance tests to be made for the interactions between pilots, configurations and/or blocks, using a fixed-effects model (Figure 12).

The application of these techniques to pilot rating data is discussed in (5). It is suggested in that reference that rating data be, in a manner of speaking, pre-whitened to standardize the variance prior to application of these techniques. However, the transformation indicated for this purpose is effective only for ratings below 3 and above 8 and was not applied in the current study, which has relatively few ratings in these ranges.

Analysis of variance techniques were applied to each of the pilot rating blocks of Figure 13. In the small STOL aircraft study, where seven manual control blocks were examined, a joint analysis of these blocks was also undertaken. In this case a weighted analysis of variance was required to cope with the combination of factorial and balanced-incomplete-block designs and the analysis was restricted to data within these basic designs to avoid undue computational difficulties. The two powered control cases from the small aircraft study were also examined in a joint analysis of variance.

True error estimates for this analysis could only be obtained from the relatively few replicated points with the result that only the joint analyses provided useful interaction tests.

The results of this analysis can be summarized as follows:

1. The best estimate of the intra-pilot variance was $\sigma^2 = 1.07$, though variations in this value from block to block were unaccountably large.
2. Pilot effects (inter-pilot variations) were statistically significant* in each instance and were reasonably consistent from block to block.
3. Configuration effects (variations between the primary non-linear control combinations) were also highly significant. Since these effects represent the pilot ratings corrected for pilot effects and interactions, they form the basis for the response surface analysis. The fact that these effects were significant meant that a response surface analysis was clearly warranted.
4. Block effects (variations between block parameters) could only be deduced from the joint block analyses. In the small aircraft manual control study, block effects were highly significant, suggesting that at least some of the parameters varied had an appreciable influence on pilot rating. The block effects from the powered control analysis were not quite significant but the response surface comparisons which follow make it difficult to rule out a real though relatively small difference between the two powered control blocks.
5. Last, but not least, there was no evidence in either the individual or joint block studies of significant second or third order interactions between pilots, configurations and block parameters. The absence of configuration x block interactions implies that the only difference between blocks in the joint analyses lies in an adjustment to the overall block mean, i.e. that the effect of a change in block parameter is an increment in rating which is independent of the test configuration. This result is extremely useful in that it suggests that a response surface fitted to the data would have the same basic shape for all blocks within the group. Moreover, it suggests that pilot rating results obtained as a function of any one block parameter, e.g. turbulence level or control friction, for a single linear or non-linear control configuration, could be applied to any other non-linear control configuration.

The pilot and block effects for the seven small aircraft manual control blocks are presented in Figure 14. The spread between pilots constitutes about 1.2 rating points and the inter-pilot variance was estimated at $\sigma_p^2 = 0.25$ or about one quarter of the intra-pilot variance. Most of the inter-block variation is accounted for by the control friction effects on pilot rating; 5 lb. of friction amount to a pilot rating degradation (measured from the basic block) of ~ 1.5 rating points. The increased turbulence (+ gust) and increased dihedral blocks account for most of the remaining variation. Both effects produced a pilot rating degradation of about 0.35 rating points from the basic block.

As a final check on the adequacy of the fixed-effects model which constituted the basis of the foregoing analysis, normality checks were performed on the rating residuals. The results for the basic small aircraft manual control block are illustrated in Figure 15 in the form of a cumulative frequency polygon. The standard normal distribution function F(t) is also shown and 95% confidence bands for F(t) are provided for the given sample size N, as a guide to interpretation of the polygon (6). Since the measured results lie within the prescribed confidance bands, the data is consistent with the normal distribution hypothesis. This data was also subjected to a χ^2 test for goodness of fit to the normal distribution (7) and no evidence of non-normality was revealed in these tests. It appears, as a result, that the fixed-effects model adequately accounts for the primary (non-random) sources of variation.

*Results which differ at the 5% (or less) significance level are regarded as significantly different.

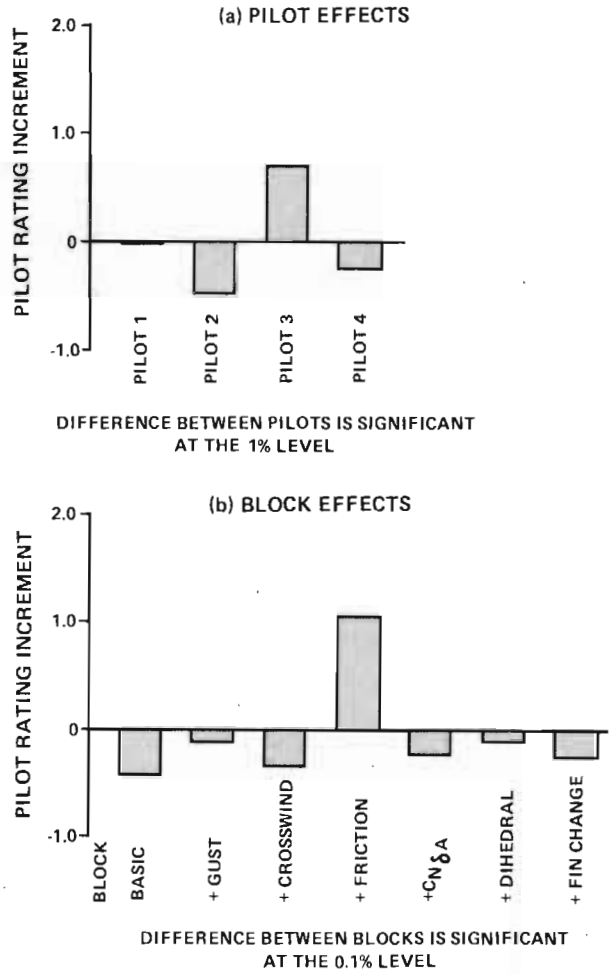

COMPARISON OF PILOT AND BLOCK EFFECTS
- SMALL STOL AIRCRAFT, MANUAL CONTROL

FIGURE 14

It should be emphasized, however, that the above comments are strictly applicable only to the range of parameters varied. It is entirely conceivable that some of these remarks are invalid outside this test range.

Response Surface Analysis of Pilot Ratings

Having isolated the configuration effects, polynomial regression techniques were applied to define the variation in pilot rating with the primary "configuration" parameters (wheel force, roll acceleration and actuator gain non-linearities).

The analysis was faciliated by the absence of configuration x block interactions in the small aircraft studies. This meant that all seven manual control blocks could be combined in a single (more precise) response surface analysis as could the two powered control blocks. The medium STOL aircraft block was of course treated independently.

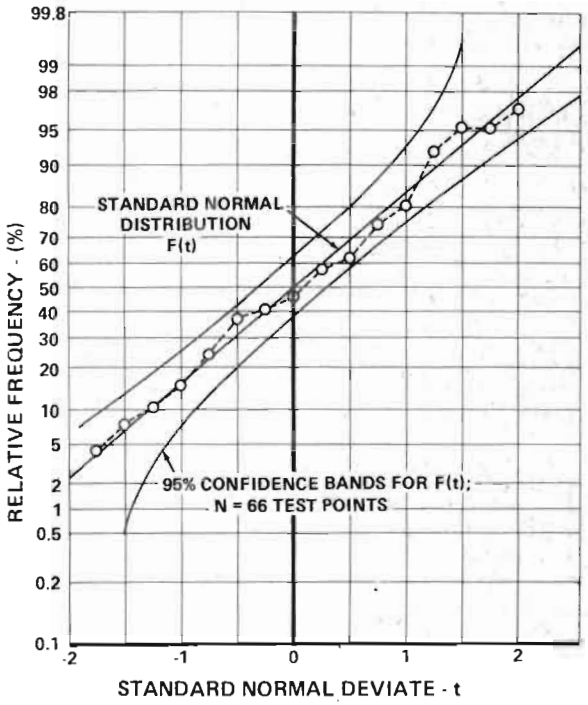

CUMULATIVE FREQUENCY POLYGON FOR THE PILOT RATING RESIDUALS
SMALL STOL AIRCRAFT
- BASIC MANUAL CONTROL BLOCK

FIGURE 15

The coordinates chosen for the response surface fit were the logarithms of the initial (inverse) wheel force and roll acceleration gradients in the manual studies (log $d\theta_w / dF_w$, log $d\ddot{\Phi}_o / d\theta_w$) and the logarithms of the actuator gain (log $1/T$) and initial roll acceleration gradients in the powered studies. These coordinates were arrived at by trial and error, in an effort to determine the parameters which both minimized the lack of fit for a given equation and resulted in the lowest order (simplest) response surface. (The choice of initial gradient as a parameter for each non-linearity was based on the results of (8) which suggest that, given adequate roll power for the task at hand, pilot opinion is a function only of roll sensitivity.)

A variety of regression techniques was applied in the course of this study to arrive at a "Best Regression" equation for each set of data (see (9) for a summary of techniques). Blind adherence to any one technique was impractical and undesirable and in the end the choice of a best fit was based on a combination of analysis and engineering judgment.

Ultimately it was determined that 90% of the variation in pilot rating about the mean could be accounted for with a two-dimensional quadratic fit in all manual control cases and with a one-dimen-

sional quadratic fit (in the log $d\ddot{\Phi}_o/d\theta_w$ direction) in the powered cases.

This fact is illustrated in Figure 16 where the "multiple correlation coefficient R^2" is plotted as a function of the response surface fit. Clearly linear fits were inadequate and little gain in prediction accuracy could be expected from cubic or higher order regression models in each case.

The quadratic response surface results for the small and medium STOL aircraft with manual controls are presented in Figure 17. The pilot ratings shown for the small aircraft represent the configuration effects averaged over all manual control blocks plus the "basic" block mean. The medium aircraft ratings are also mean plus configuration effects.

A comparison of the small and medium aircraft contours indicates that, outside of a shift in the $d\ddot{\Phi}_o/d\theta_w$ coordinate, there is no (statistically) significant difference between the two sets of contours. The optimum wheel force gradients are essentially the same ($dF_w/d\theta_w$=20 lb/rad.). The optimum roll acceleration gradients ($d\ddot{\Phi}_o/d\theta_w$=2.2 rad/sec.^{2} and 0.64 rad/sec.^{2}) are approximately inversely proportional to the aircraft TR's (Table 1) and use is made of this fact in a subsequent section. The optimum in each case closely approximates the linear wheel force and roll acceleration characteristics. (Curve 4 of Figure 9 is the closest we come to a linear roll acceleration characteristic in this study.) The pilot tolerates a wide range of non-linearity in the wheel force or roll acceleration with little degradation in pilot opinion. However, his choice of (optimum) wheel force gradient is a function of the roll acceleration gradient and vice-versa. This is illustrated by the diagonal lines of Figure 17(a)

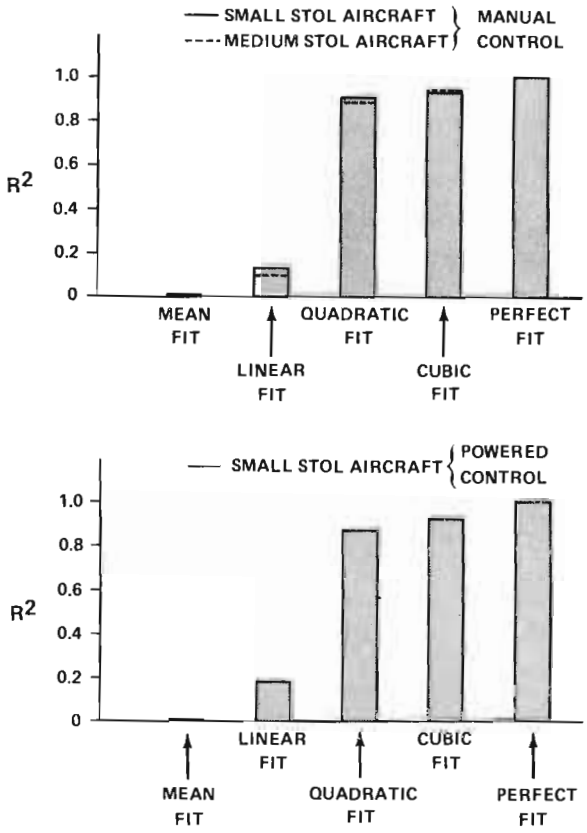

THE MULTIPLE CORRELATION COEFFICIENT (R^2) AS A FUNCTION OF THE RESPONSE SURFACE MODEL

FIGURE 16

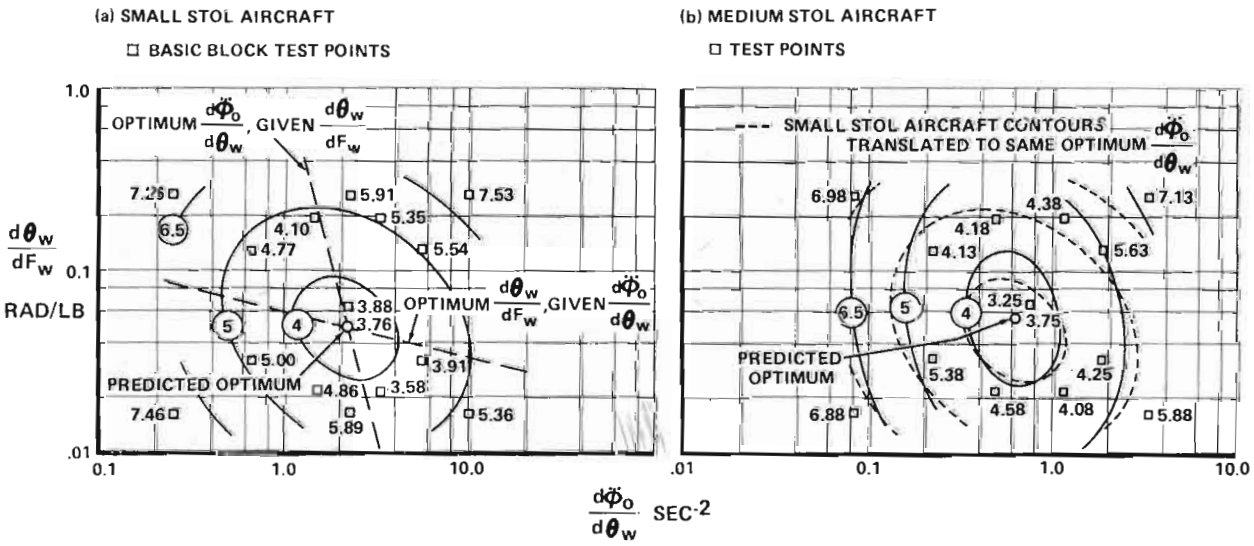

PILOT RATING RESPONSE SURFACE CONTOURS
MANUAL CONTROL

FIGURE 17

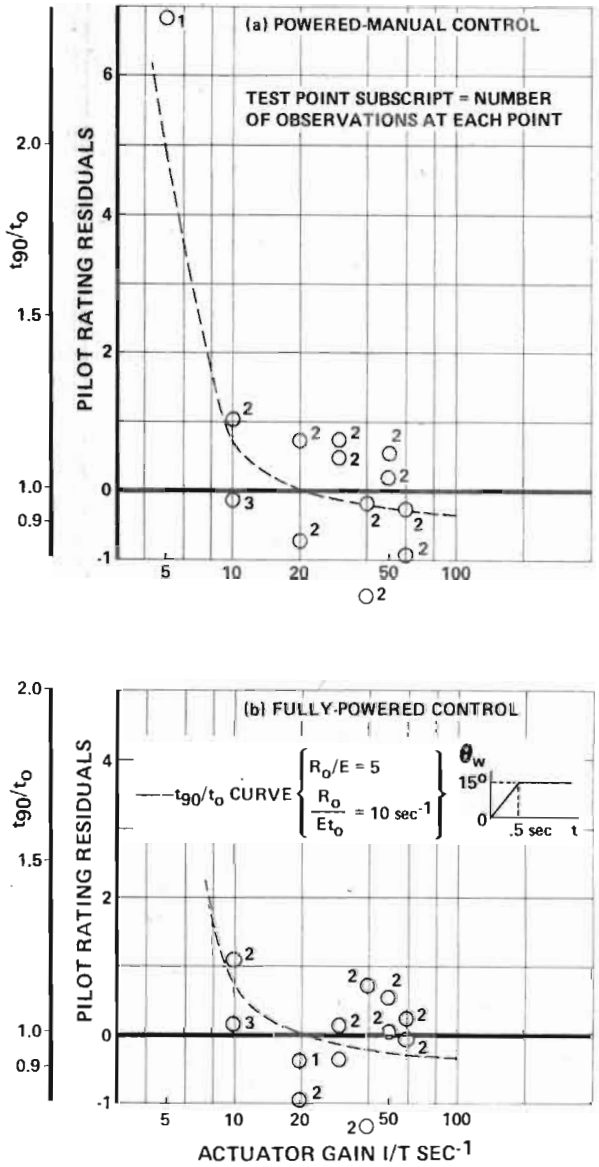

PILOT RATING RESIDUALS AS A FUNCTION OF ACTUATOR GAIN

FIGURE 18

which indicate that he chooses higher wheel force gradients as the roll acceleration gradient is increased and conversely higher roll acceleration gradients as wheel forces are increased.

Since the powered cases employed the linear wheel force characteristic (curve D of Figure 8) used in the manual control studies, we might expect the quadratic variation in rating with $\log d\Phi_o/d\theta_w$ for these cases to be similar to that obtained from a horizontal cut of the manual response surface at the corresponding wheel force gradient. This was actually the case. However, despite the fact that a degradation in rating might be expected due to actuator lag effects, the optimum pilot rating in the fully-powered case was significantly less than that obtained in the manual control analysis, while the powered-manual optimum was statistically consistent with the manual result. These facts suggest that the control dynamics, deleted for the fully-powered studies, had a significant effect on rating, while the effects of the valve preload spring in the powered-manual simulation were insignificant.

Since most of the variation in pilot rating for the powered cases was accounted for by the quadratic log $(d\Phi_o/d\theta_w)$ variation, the influence of actuator gain could be best detected by removing this variation and examining the residuals. The results are shown in Figure 18 for both the powered-manual and fully-powered cases. It is evident that in the range $60 \geq 1/T \geq 10$, variations in residual rating with $1/T$ are slight. If, however, we introduce the $1/T = 5$ rating point heretofore neglected in the powered-manual studies (and adjust the rating of 10 to correspond to the residual rating scale) the trend with $1/T$ takes on a new light. An abrupt rise in rating with $1/T$ values below 10 seems to be indicated. Unfortunately, the experimental design was such that additional ratings in this range were not obtained.

However, it is interesting to examine this result in conjunction with a control system response analysis. The latter consisted of a simple nonlinear actuator with an arbitrary ramp input, and the time to achieve 90% (t_{90}) of output was examined as a function of $1/T$, the actuator gain. The results are shown in Figure 19 with the input ramp displacement (R_o) ramp time (t_o) and maximum valve displacement (E) as parameters. A very abrupt rise in the response time is evident from this plot below a critical actuator gain, for each R_o/E ratio shown.

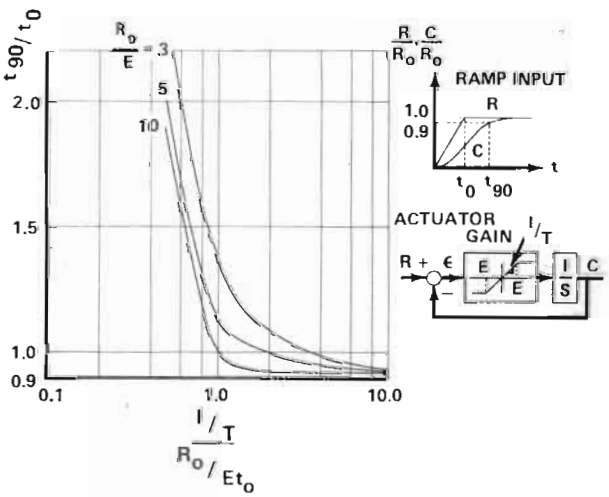

TIME TO ACHIEVE 90% OF CONTROL AS A FUNCTION OF ACTUATOR GAIN

FIGURE 19

The curve for $R_o/E = 5$ and $R_o/Et_o = 10$ sec.$^{-1}$, corresponding to a $\theta_w = 15^o$ ramp in $t_o = 0.5$ sec. for the present study, has been superimposed on the rating residual plots of Figure 18 for comparison. The response times reach $t_{90}/t_o = 2$ or twice the ramp input times at an actuator gain of $1/T = 5$ in this case and the degradation in pilot rating is consistent with this degradation in response. This tends to confirm the pilot rating trends deduced above and suggests that the foregoing ramp may be representative of pilot assessment inputs in this experiment. It is interesting to note that this ramp corresponds roughly to a sinusoidal input of 15^o amplitude at $\omega = 2$ rad/sec. The latter frequency corresponds closely to the crossover frequency familiar from pilot/aircraft transfer function studies(10).

Questionnaire Replies

The questionnaires, which the pilots completed following each evaluation (Figure 7), documented the rationale behind their pilot opinion ratings and served to explain some of the rating trends of the preceding section. Space limitations preclude tabulation of the individual questionnaire replies but the overall results can be deduced through a response surface analysis of the replies to each question.

The technique employed to obtain a response surface fit of each question is best described by an example. Consider Question 1, where three replies are possible. If we assign a score of +1 to a wheel force "too high" response, a -1 to a "too low" response and zero to no response whatever, the questionnaire replies are converted to numerical form. The results may then be treated, in the manner of rating data, by response surface techniques. The response surface contours defined by scores of ± 0.5 then represent the boundaries beyond which, on the "average", pilots object to the wheel force characteristics and between which these characteristics are generally acceptable. A similar procedure is used when only two replies are possible to a particular question.

This technique has been applied to the small and medium STOL aircraft manual control replies. In view of the results obtained from the pilot rating analysis, the questionnaire replies for the seven small aircraft blocks were considered jointly and "average" boundaries were derived.

Since the numerical scale used is coarse (only 3 levels at most) it is apparent that boundaries based on relatively few replies will be very qualitative and sometimes misleading. For this reason, questions which evoked an inadequate response were not considered in the subsequent discussion and the small aircraft results will carry considerably more weight than the medium aircraft replies which were confined to results from a single block (small sample).

The response to each question is presented in Figure 20 and discussed below. Unless otherwise indicated, these remarks will be directed at the small aircraft boundaries. In order to provide a meaningful comparison of the small and medium STOL aircraft results, the $d\ddot{\Phi}_o/d\theta_w$ coordinates in this plot have been normalized with respect to the predicted optimum values from Figure 17. Since the optimum wheel force gradients were virtually identical for the two aircraft, the original coordinates are retained in this direction.

Question 1 - Wheel Force for Small Displacements

The response surface boundaries for Question 1 show that the pilot's choice of force gradient is a function of the roll acceleration gradient, larger force gradients being desired with increasing roll response. These boundaries are parallel to the line of optimum $d\theta_w/dF_w$ given $d\ddot{\Phi}_o/d\theta_w$, from the rating results of Figure 17(a). This might be expected since the questionnaire replies define the rationale behind the pilot opinion ratings. Since the boundaries are not parallel to lines of constant $d\ddot{\Phi}_o / dF_w$ (45^o lines), pilot opinion is obviously influenced by both response per unit force and per unit displacement.

The medium and small aircraft results agree except for a shift in the "too low" boundary. It is not possible to determine whether the shift is real or is associated with the limited sample size in the former case.

Question 2 - Wheel Force for Large Displacements

The boundaries of Question 2 show dissimilar trends. While the "too low" boundary oscillates about a line of constant $d\theta_w / dF_w$ the "too high" boundary is more consistent with a line of constant $d\ddot{\Phi}_o / dF_w$. The latter effect is caused by the fact that higher wheel forces are required to achieve adequate roll power when the roll acceleration characteristics exhibit little response over centre (curves 1 and 2 of Figure 9).

The medium STOL aircraft replies yield only rough approximations to the foregoing boundaries. The discrepancies are attributed to the small sample size.

Question 3 - Roll Power for Small Displacements

The boundaries for Question 3 indicate that the pilot demands slightly higher roll accelerations with increasing wheel force gradients. We might expect these boundaries to be parallel to the line of optimum $d\ddot{\Phi}_o / d\theta_w$ given $d\theta_w / dF_w$, from the rating results of Figure 17 (a), and this is roughly the case.

The boundaries for the medium aircraft are independent of wheel force gradient, but correspond well otherwise to the small aircraft results.

Question 4 - Roll Power for Large Displacements

The boundary defining "high" roll powers for large displacements is located at low values of $d\ddot{\Phi}_o / d\theta_w$ where the non-linearities exhibit a low response over centre followed by a very rapid response near $\theta_w = 30^o$ (curves 1 and 2 of Figure 9). This rapid response has a gradient similar to that which the pilot encounters at small wheel angles with curves 6 and 7 of Figure 9, and which he regards (Question 3) as unacceptable; hence his complaint. The low wheel forces aggravate the situation since the larger wheel deflections are more readily obtained. Apparently he recognizes the decrease in roll acceleration gradient with large wheel angles in curves 6 and 7 and retracts his over-centre response complaint for these configurations.

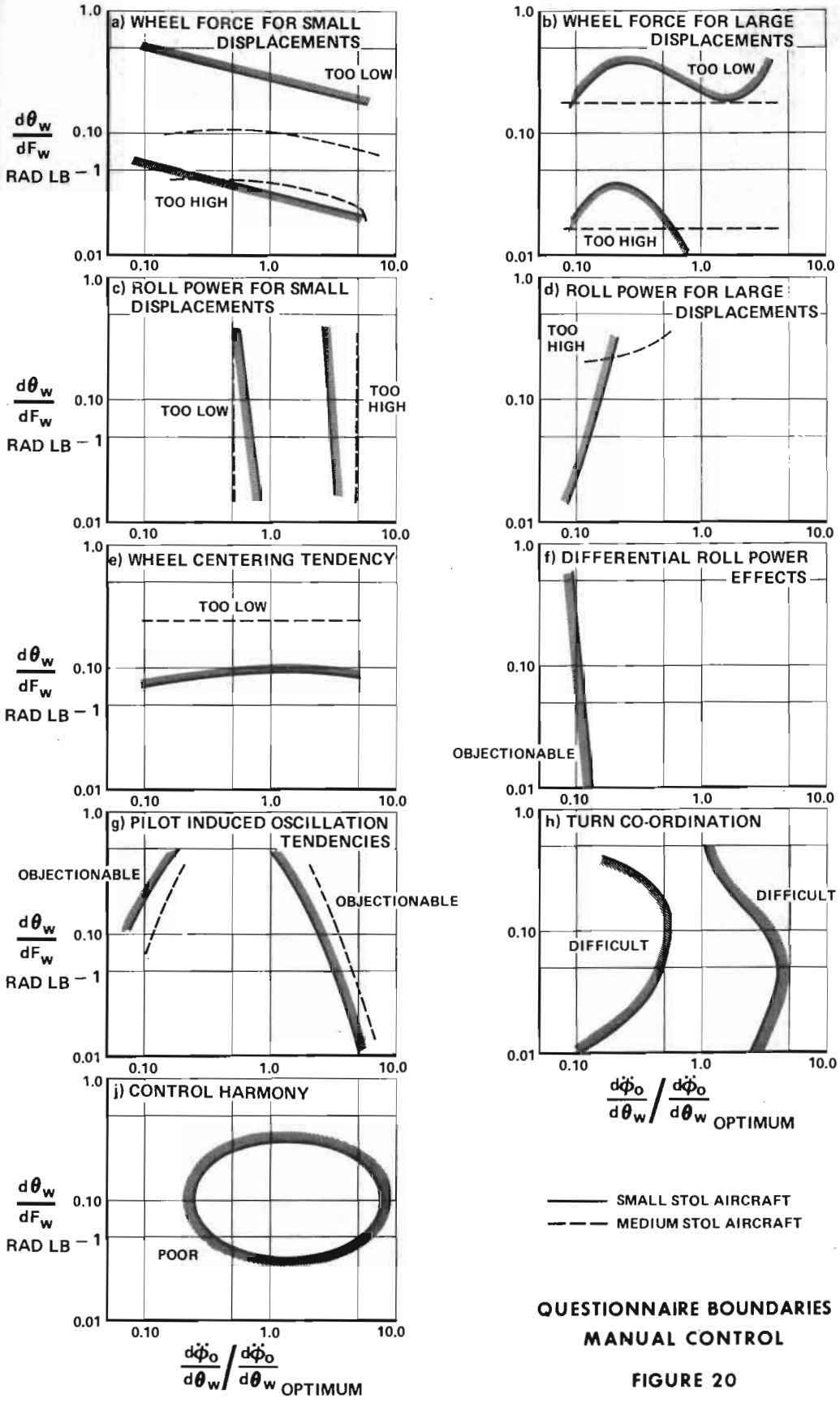

QUESTIONNAIRE BOUNDARIES
MANUAL CONTROL

FIGURE 20

Question 5 - Wheel Centering Tendency

The replies for the small aircraft show that poor wheel centering results from wheel force gradients below 10 lb/rad., independent of the roll acceleration gradient, while the corresponding boundary for the medium STOL aircraft is located at 4 lb/rad. This difference is attributed to the fact that the small aircraft experiment included a 5 lb. control friction block, while the medium aircraft control system was frictionless; the 4 lb/rad. value can be considered adequate only in the unlikely event that no control friction is anticipated.

Question 9 - Differential Roll Power Effects

"Differential Roll Power Effects" began to appear with curve 1 of Figure 9. As a result of the low initial slope of this curve, the wheel travels required to hold sideslip or crosswinds are large and the pilot often finds himself "trimmed" near mid travel where the roll acceleration gradient rises abruptly. Wheel travel increments above "trim" then induce a very fast roll response, while decrements in wheel travel produce little response, and the pilot comments reflect these differential effects.

Question 14 - Pilot Induced Oscillation Tendencies

The pilot induced oscillation boundaries of Figure 20(g) evoke particular interest since the PIO problem is amenable to theoretical analysis. It is possible then to associate the experimental results with theory.

Consider first the analytical problem. For a linear lateral control system, it is generally recognized (11) that unless $\omega_\phi / \omega_d > 1.0$ in the ϕ/δ_A transfer function and the damping ratios ζ_ϕ and ζ_d are relatively low, a sustained oscillation in roll cannot be supported. The small and medium STOL aircraft of this study have an $\omega_\phi / \omega_d < 1.0$ and a relatively high ζ_ϕ and ζ_d (Table 1), so that these aircraft would not ordinarily be susceptible to PIO. However, it was noted earlier that by virtue of the time required to tilt the helicopter rotor, a 0.1 sec. lag was effectively introduced in the roll control simulation. This lag (which is considered representative of aircraft spoiler lags) when incorporated in the ϕ/δ_A transfer function, provides the mechanism for PIO.

This fact is illustrated in Figure 21 where the Nyquist plots ($Y_p \cdot Y_c(\omega)$) for the small and medium STOL aircraft are shown. The pilot describing function has been represented as a pure gain $Y_p = K_p$ in these plots (11) and the aircraft transfer function has been approximated by:

$Y_c = \dfrac{K_C T_R e^{-0.1s}}{s(T_R s + 1)}$. The latter expression constitutes an adequate representation of these aircraft in the frequency range of interest (i.e. when $\omega/\omega_d > 2$; $|T_s| > 20$ sec.-see Table 1). An arbitrary gain $K_p K_c = 10$ has been used in both plots since the pilot gain is not known. The roll acceleration non-linearities of Figure 9 have been normalized ($\ddot{\Phi}/\ddot{\Phi}_{max}$ vs $\theta_w/\theta_{w\,max}$) and replaced by their

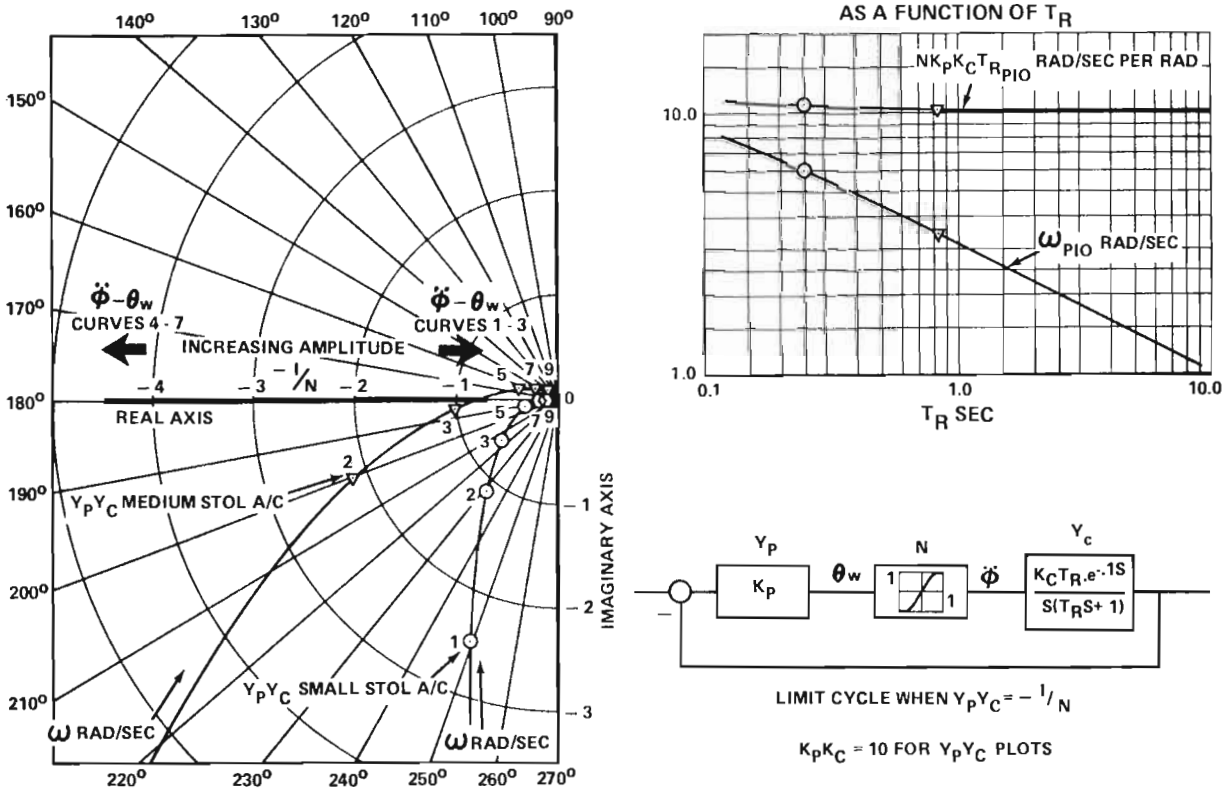

PILOT INDUCED OSCILLATION PREDICTIONS

FIGURE 21

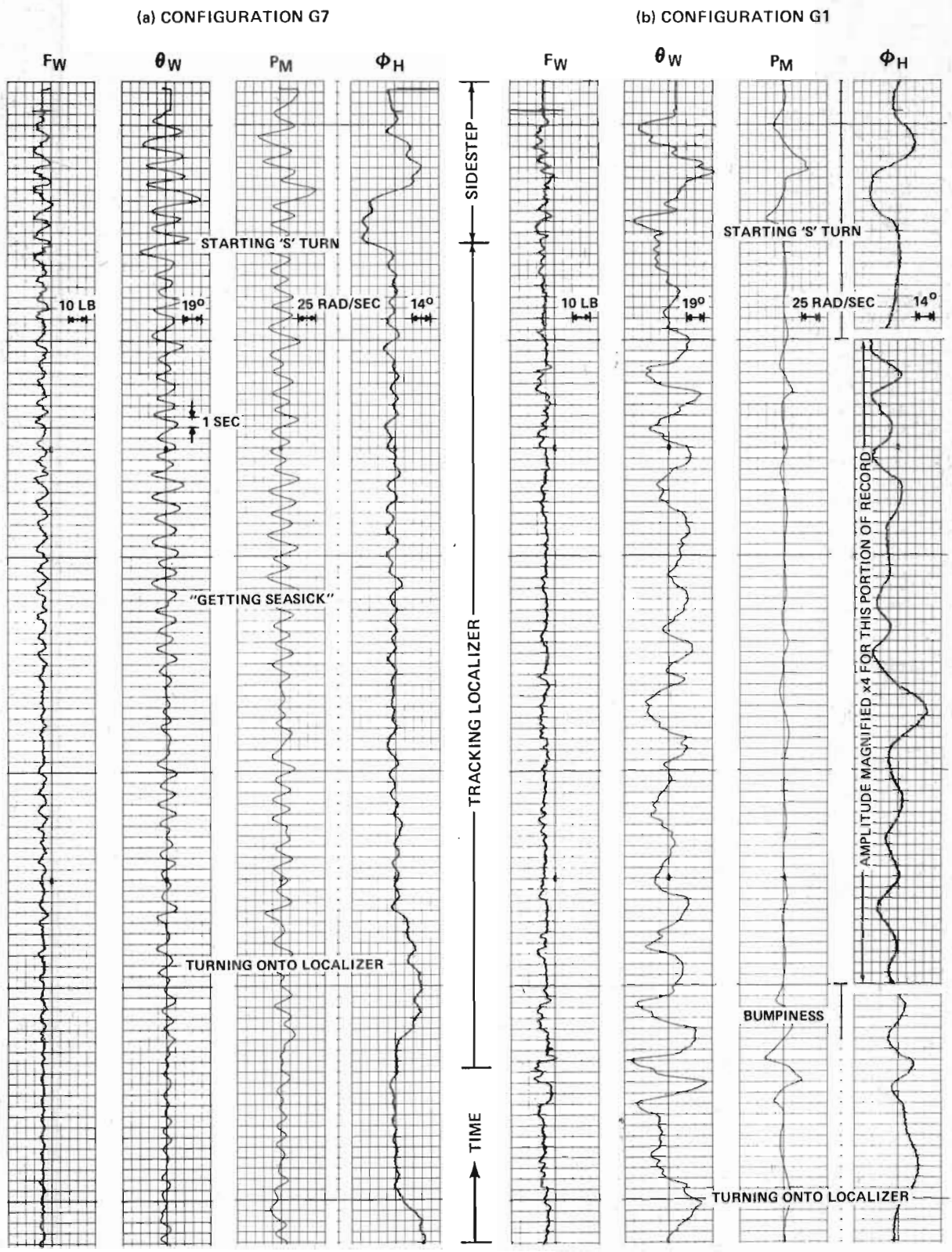

'PILOT INDUCED OSCILLATION' RECORDS MEDIUM STOL AIRCRAFT - PILOT 1

FIGURE 22

equivalent linear gains "N" from single sinusoidal-input describing function theory [12]. The equivalent gains are functions of amplitude, reducing to unit equivalent gain in the linear case.

Pilot induced oscillations in the form of a limit cycle are predicted when the $Y_p Y_c$ (ω) transfer function intersects the $-1/N$ equivalent gain trajectory on the negative real axis of the Nyquist diagram. Clearly, if the pilot gain is sufficiently high, a limit cycle will result for this simulation. Whether this limit cycle is stable or not, however, depends on the direction of $-1/N$ with increasing amplitude. Non-linearities 4 - 7 of Figure 9 generate stable limit cycles while curves 1 - 3 result in unstable limit cycles for wheel amplitudes less than $\theta_w = 40^o$.

The gains required for PIO and the predicted PIO frequencies, are shown in the upper right-hand corner of Figure 21 as a function of T_R. According to this theory the controlled-element gain K_C required to sustain PIO varies approximately with $1/T_R$ for a given non-linearity N and pilot gain K_p, and the PIO frequencies for the small and medium STOL aircraft should be $\omega = 6$ rad/sec. and $\omega = 3.4$ rad/sec. respectively.

The predicted frequencies are in fact corroborated by experiment. A typical PIO record for medium aircraft configuration G7 is shown in Figure 22(a) and has a frequency of 3.3 rad/sec. The oscillation amplitude is $\theta_w \sim 10^o$, $\Phi \sim 4^o$ and the 180^o phase angle between θ_w and Φ confirms the assumption that the pilot is acting as a pure gain ($K_p \sim 2.5$ rad/rad.). The results of Figure 20(g) reflect this PIO in that configuration G7 is well within the PIO region. However, the PIO boundary is not independent of force gradient as the above considerations might suggest. Instead PIO tendencies diminish with increasing force gradient. This is in fact a recognized way of alleviating PIO, [13], and indicates that the pilot's gain decreases with increasing wheel forces.

Figure 20(g) also reveals a PIO tendency which would not be anticipated from the foregoing considerations. This "PIO" is recorded near configuration G1 where the forces are low and the roll acceleration non-linearity takes on the features of a "deadband". A typical record of this oscillation is shown in Figure 22(b) for the medium STOL aircraft. The frequency is low, about 0.9 rad/sec. and the wheel and bank angle amplitudes are approximately 20^o and 4^o respectively. A stable limit cycle is possible in theory at or near the dutch roll frequency ($\omega_d = 0.894$ rad/sec.) with this "deadband" characteristic, if we postulate sufficient pilot lag [14]. However, it is difficult to state conclusively that this PIO was encountered by the pilots. Interpretation is confused by the dutch roll excitation due to turbulence and the obvious difficulty the pilot has in coping with this excitation when the roll control is so inadequate (witness the "bumpiness" comment in Figure 22(b) and the resulting pilot control attempts).

Finally, we note that the small and medium STOL aircraft boundaries are in good accord.

Question 16 - Turn Coordination

Difficulties in turn coordination were noted by the pilots under two conditions; where a very low initial response gradient was followed by a very steep gradient (curves 1, 2 of Figure 9), and where the initial response gradient was high (curves 6, 7 of Figure 9). Some relief from turn coordination difficulties was experienced at the higher wheel force gradients. The higher forces make it more difficult for the pilot to "overcontrol".

Question 17 - Control Harmony

The boundaries for this question illustrate the fact that control harmony is a question of matching both the response and force characteristics of the aircraft controls. The wheel force gradient for best control harmony is 10 lb/rad. which is lighter than the overall optimum suggested by the pilot rating results of Figure 17 ($\sim$20 lb/rad.). However, this is consistent with the fact that both rudder and elevator force gradients were light in the simulated aircraft.

An interesting result has emerged from the analysis of the questionnaires. In both the small and medium STOL aircraft plots, the abscissa for the questionnaire boundaries was roll acceleration gradient non-dimensionalized by the optimum value of this gradient. Plotted in this manner, the boundaries for these aircraft are virtually superimposed. The optimum roll acceleration gradients on the other hand vary approximately with $1/T_R$, according to the pilot rating results of Figure 17. This indicates then that both the questionnaire and pilot rating boundaries shift with $1/T_R$. This fact is supported by the theory for Question 14, and provides the basis for an extension of the results of this study in the next section.

VIII PROJECTION OF RESULTS

If we assume an aircraft transfer function of the form: $Y_c = \dfrac{K_C T_R e^{-0.1s}}{s(T_R s + 1)}$

implying closed loop control of bank angle with little more than nuisance dutch roll effects [15], large spiral times ($|T_s| > 10$-20 sec.), and a 0.1 sec. spoiler lag, then the small and medium STOL aircraft results of the preceding sections yield the variation in pilot opinion with system gain K_C (non-linear control elements) for two widely separated values of roll mode time constant T_R (0.25 and 0.83 sec. respectively).

In view of this T_R spread, we are in a position to speculate on the nature of pilot rating variations with T_R and at this point it is useful to compare the current data with results from the available literature.

The effect of system gain K_C on pilot opinion is shown in Figure 23 for the two STOL aircraft of this study and for the ground-based simulations of [8] and [16] respectively. (The Reference 16 data is derived from a longitudinal simulation but the results are included as a matter of interest.)

K_C is taken as $d\ddot{\Phi}_o / d\theta_w$, the roll acceleration gradient over centre, in the current studies

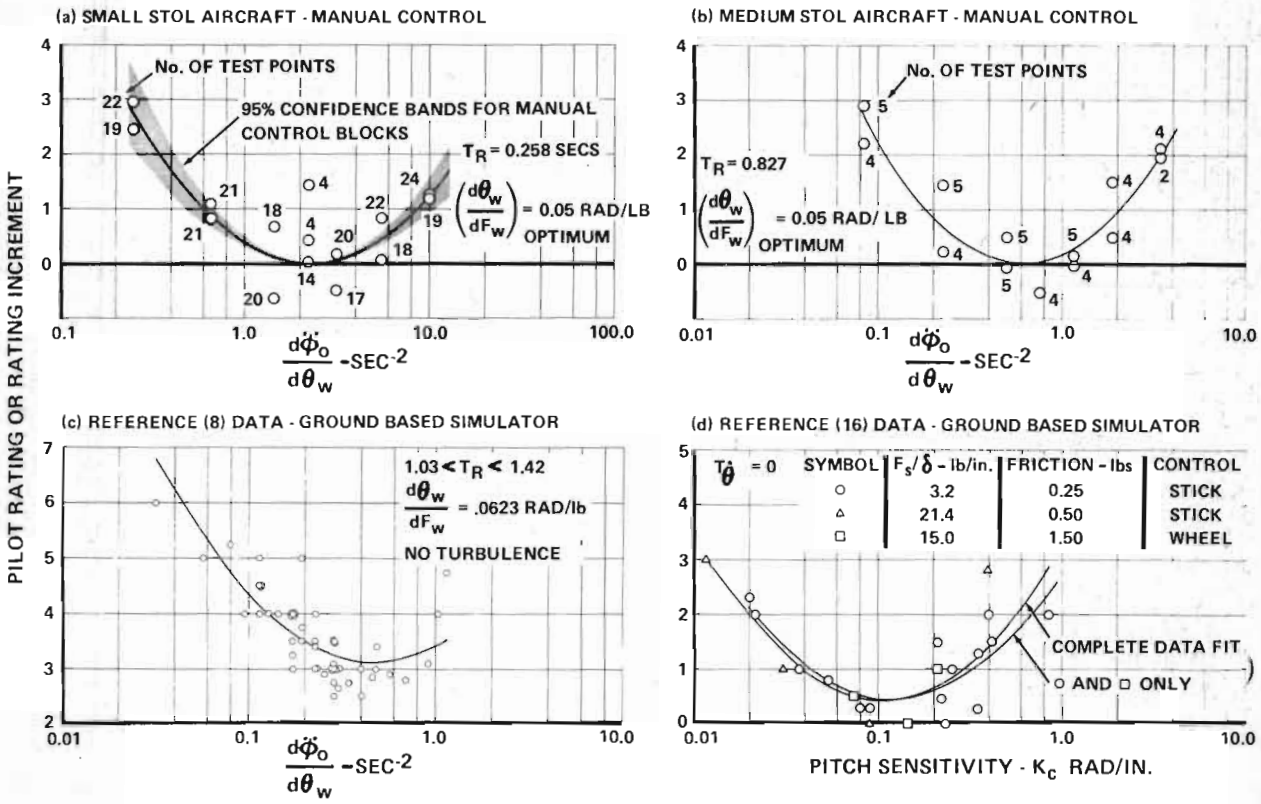

VARIATION IN PILOT RATING WITH SYSTEM GAIN FOR THE CURRENT STUDY AND TWO GROUND BASED SIMULATOR STUDIES

FIGURE 23

and the fitted curves derive from a cut through the pilot rating contours of Figure 17 at the optimum wheel force gradient. The results are plotted as deviations from the optimum rating. A measure of the variation between the 7 manual control blocks of the small STOL aircraft study is provided by the 95% confidence bands on the fitted curve.

The corresponding results from (8) were obtained for a 500,000 lb. aircraft (moving-base) simulation with non-linear roll controls, performing a flight task similar to that used in the current study. A quadratic fit of this rating data in the range $1.03 < T_R < 1.42$ is shown in Figure 23(c) and considering the sparsity of data at high K_C's, constitutes a reasonable representation of the results.

The K_C of (16) is pitch control sensitivity and the results derive from a VTOL aircraft (fixed-base) simulation. The task was to hold the airplane level in the presence of turbulence. The pitch mode time constant, analogous to T_R in the lateral simulations, was taken as zero in this part of the study. A quadratic fit of the data shown in Figure 23(d) provides a good representation of the results despite variations in stick force gradient. The results represent deviations from the optimum rating of (16).

A comparison of the fitted pilot rating curves for these four simulations is shown in Figure 24. Despite wide variations in the simulated aircraft (T_R in particular) and control (wheel force etc.), characteristics and even appreciable deviations in flight task, there is little difference between the pilot rating curves. To a first order the pilot rating for a given T_R varies as $(\log K_C/K_{C\,opt})^2$; though this expression must break down in the limit as the absolute pilot ratings approach 1 or 10.

While the shape of the pilot rating vs K_C characteristic is apparently unaffected by T_R, the value of K_C which optimizes pilot rating (i.e. K_{Copt}) depends primarily on T_R(10) (17). Reference 10 suggests a form for this variation based on the hypothesis that the pilot gain in the crossover region is the pilot's chief concern. The results seem to correlate well with VTOL data when the magnitude of the pilot describing function $|Y_P|$, rather than the static pilot gain K_P is used to generate the variation with T_R. The important difference between these two is the pilot lead T_L

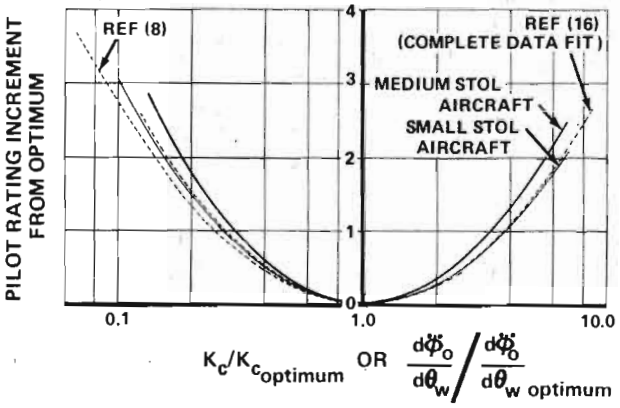

COMPARISON OF THE VARIATION IN PILOT RATING WITH SYSTEM GAIN

FIGURE 24

which is a function of T_R. Unfortunately, the $|Y_p|$ model is not consistent with the present results and we will postulate that K_p at crossover is the pilot's chief concern. Then, at crossover, by definition $|Y_p(\omega_c) \cdot Y_c(\omega_c)| = 1$ whereby -

$$|Y_p(\omega_c)| = 1/|Y_c(\omega_c)| = \omega_c\sqrt{T_R^2\omega_c^2 + 1}\Big/K_CT_R$$

but

$$|Y_p(\omega_c)| \propto K_p\sqrt{T_L^2\omega_c^2 + 1} \text{ where } T_L = T_L(T_R)$$

and if we consider ω_c to be roughly constant, then a line of "best opinion" will be defined by:

$$K_CT_R \propto \frac{\omega_c}{K_p}\frac{\sqrt{T_R^2\omega_c^2 + 1}}{\sqrt{T_L^2\omega_c^2 + 1}}$$

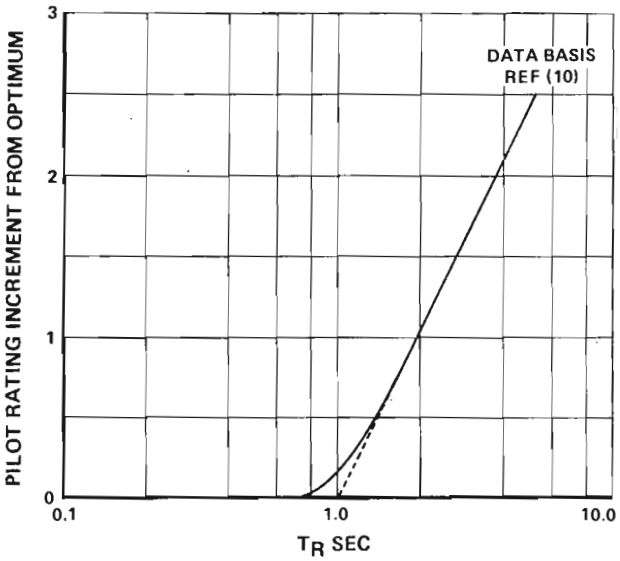

VARIATION IN PILOT RATING WITH T_R AT OPTIMUM PILOT GAIN

FIGURE 25

For a constant K_p and the variation in lead T_L with T_R, presented in (10), this relation defines a K_CT_R value that is relatively insensitive to both T_R and ω_c. The result is shown in Figure 26 (optimum pilot gain curves for ω_c = 1.5, 2.5 rad/sec.) along with the optimum K_CT_R values for the present STOL aircraft and the Reference 8 studies. The correlation between the postulated model and these experiments is seen to be very good. To a first order then the pilot seeks an optimum roll rate gradient

$$d(\ddot{\phi}_o T_R)/d\theta_w = dp_o/d\theta_w = 0.55 \text{ rad/sec/rad.}$$

independent of T_R, for these aircraft. This is consistent with the conclusion that $K_{C\text{optimum}}$ is proportional to $1/T_R$, deduced from the questionnaire replies of the previous section.

Although the generation of lead equalization T_L, with increasing T_R, is essential to the achievement of satisfactory closed loop control, it is not obtained without penalty. The generation of lead, even with an optimum pilot gain, manifests itself in a degradation in pilot opinion. Figure 25 shows this degradation in pilot rating plotted against T_R

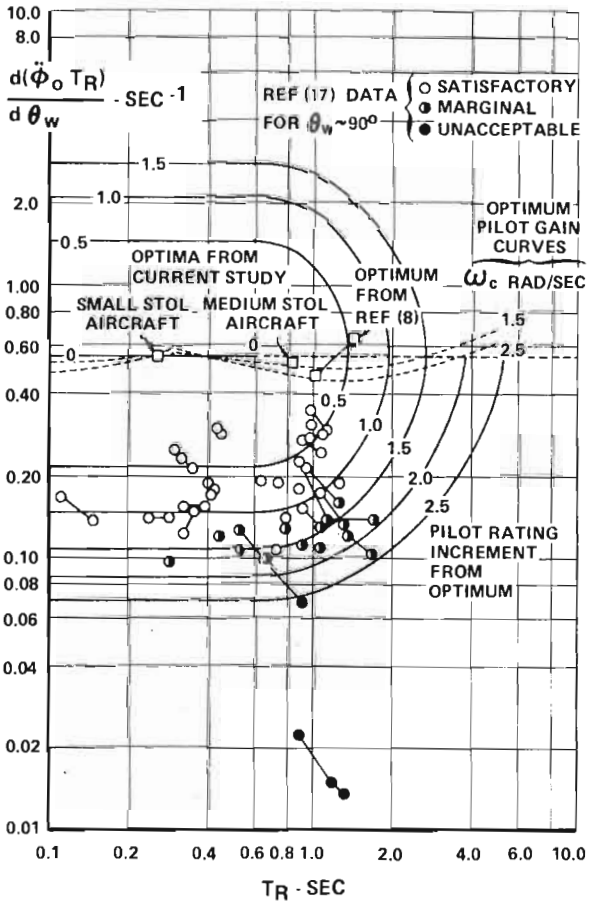

PILOT RATING INCREMENT AS A FUNCTION OF ROLL RATE GRADIENT AND T_R

FIGURE 26

(rather than T_L) for the optimum pilot gain. This result was selected from the data and considerations of (10).

In summary then the variations in pilot rating with K_C and T_R are as follows:

1. The pilot rating variation with K_C is approximately proportional to $(\log K_C/K_{C_{opt}})^2$, independent of T_R, (Figure 24).
2. The optimum system gain and best pilot opinion line is defined as a function of T_R by the relation $K_C T_R = d(\ddot{\phi}_o T_R)/d\theta_w$ = constant.
3. Pilot rating degenerates with T_R, along the optimum gain line, because of pilot lead requirements (Figure 25).

These results can now be employed to generate pilot rating contours as a function of K_C and T_R. Contours will be plotted as pilot rating increments from the optimum pilot rating since comparisons were made on this basis.

The final result is shown in Figure 26. This figure is strictly applicable only for the optimum wheel force gradient (20 lb/rad.), but changes in wheel force gradient cause little more than a slight vertical shift in the contours (note the optimum $d\ddot{\phi}_o / d\theta_w$ line given $d\theta_w/dF_w$ in Fig.17(a)).

Efforts to incorporate miscellaneous STOL aircraft rating measurements, e.g. (18), in Figure 26, were hampered by the fact that rating increments from optimum are seldom determined and there is often the conversion from one of several stick-type controls to the wheel-type control to contend with.

Nevertheless, a qualitative check on the rating trends shown here is provided by the data of (17) for large transport aircraft. This data divides pilot opinion into three categories, satisfactory, marginal and unacceptable, as shown in Figure 26. It is difficult to interpret these definitions in terms of the present rating scale, but we note that the dividing line between categories follows, remarkably well, the trend indicated by the current rating contours.

IX CONCLUDING REMARKS

An attempt has been made in this study to define the effects of control non-linearity on the lateral handling qualities of STOL aircraft during approach. This investigation has resulted in the following conclusions:

1. A statistical analysis of the pilot ratings revealed that pilot bias was highly significant, a fact which suggests that experimental designs for programs of this type should permit the isolation and elimination of these effects. Interactions between pilots and aircraft or control configurations were, on the other hand, insignificant in this study.
2. A response surface analysis of the "manual control" rating data suggests a quadratic variation in pilot rating with the logarithm of the initial wheel force and roll rate $d(\ddot{\phi}_o T_R)/d\theta_w$ gradients of the non-linearities. This fact has culminated in a set of STOL aircraft pilot opinion boundaries as a function of the aircraft roll mode time constant and the initial roll rate gradient.
3. The few "powered control" results obtained indicate that spoiler actuator gains $(1/T) > 10$ sec.$^{-1}$ have little effect on pilot opinion while ratings degenerate rapidly for lower values of $1/T$. The influence of a spoiler valve preload spring on pilot rating was not discernable from these results.
4. A response surface analysis of the questionnaire replies served to substantiate the rating results and aptly demonstrated the power of the questionnaires in defining the basis for pilot opinion variations.

The rating results of this study are generally presented as deviations from an "optimum" rating value. This makes the correlation of these results with isolated measurements difficult; however the objective has been to identify the underlying trends in rating with various control and aircraft characteristics and the accurate definition of these trends was often inconsistent with the use of an absolute rating scale.

It is evident that the "initial gradients" may not describe non-linearities far removed from those employed in this study or the handling qualities associated with such non-linearities. In fact, a good deal of care is required in extrapolating any of the conclusions or results of this study to configurations outside the basic designs assessed.

X REFERENCES

1. Daw, D.F.; McGregor, D.M. "Development of a Model-Controlled V/STOL Airborne Simulator" NRC, NAE Aero. Report LR-352, National Research Council of Canada, February, 1968
2. Daw, D.F.; Lum, K.; McGregor, D.M. "Description of a Four Degrees of Freedom, V/STOL Aircraft, Airborne Simulator" NRC, NAE Aero. Report LR-499, National Research Council of Canada, February, 1968
3. Howard, J.; Ridler, D.A. "Assessment of the NAE Airborne Flight Simulator as a STOL Research Facility" DHC-DIR 68-4 March, 1968
4. Cockran, W.G.; Cox, G.M. "Experimental Design" John Wiley & Sons. Inc., 1950
5. Madill, D.R. "Discussion for AGARD Flight Mechanics Panel Specialists' Symposium" NASA Ames Research Center, March 10 - 13, 1970

6. Madill, D.R. "Confidence Bands for the Cumulative Frequency Polygon" DHC 70-7, June, 1970

7. Argentiero, P.D. Tolson, R.H. "A New Method of Testing Small Samples for Goodness of Fit to Normal Populations" NASA TN D-4405 October, 1966

8. Condit, P.M. Kimbrel, L.G. Root, R.G.Z. "Inflight and Ground-Based Simulation of Handling Qualities of Very Large Airplanes in Landing Approach" NASA CR-635, October, 1966

9. Draper, N.R. Smith, H. "Applied Regression Analysis" John Wiley & Sons. Inc., January, 1967

10. Ashkenas, I.L. "A Study of Conventional Airplane Handling Qualities Requirements" Part I - Roll Handling Qualities, U.S. AFFDL TR 65-138 November, 1965

11. Ashkenas, I.L. et al "Pilot Induced Oscillations: Their Cause and Analysis" Norair Report NOR 64-143, June, 1964

12. Gibson, J.E. "Nonlinear Automatic Control" McGraw-Hill Book Company, 1963

13. A'Harrah, R.C. Siewert, R.F. "Pilot Induced Instability" AGARD Flight Mechanics Panel Specialist Meeting on "Stability and Control", Cambridge, England, September, 1966

14. Barnes, A.G. Ormerod, M. "The Effect of a Dead-Space on the Lateral Control Loop" UK S & T Memo 5/68, May, 1968

15. Ashkenas, I.L. "A Study of Conventional Airplane Handling Qualities Requirements" Part II - Lateral Directional Oscillatory Handling Qualities - U.S. AFFDL TR 65-138, November, 1965

16. Lollar, T.D. "A Rationale for the Determination of Certain VTOL Handling Qualities Criteria" AGARD Report 471, July, 1963

17. Bisgood, P.L. "A Review of Recent Research on Handling Qualities, and Its Application to the Handling Problems of Large Aircraft" Parts 1 & 2, UK ARC R & M 3458, 1964

18. Innis, R.C. Holzhauser, C.A. Quigley, H.C. "Airworthiness Considerations for STOL Aircraft" NASA TN D-5594, January, 1970

XI SYMBOLS

C	spoiler actuator output
C_{l_β}	rolling moment coefficient due to sideslip
$Cn_{\delta A}$	yawing moment coefficient due to spoiler/aileron deflection
d	differential operator
$d\theta_w/dF_w$	inverse initial wheel force gradient
$d\ddot{\Phi}_o/d\theta_w$	initial roll acceleration gradient
E	maximum valve displacement
FW	wheel force (one hand)
FW_o	spoiler actuator valve spring preload
K_C	controlled-element gain
K_p	pilot static gain
N	equivalent gain of a non-linearity
p_o	steady state roll rate
p_M	roll rate of simulated aircraft "model"
R	spoiler actuator valve input
R^2	multiple correlation coefficient = Regression sum of squares about the mean/total sum of squares about the mean
T	spoiler actuator time constant
T_R	roll mode time constant
Ts	spiral time
x	$\log (d\ddot{\Phi}_o / d\theta_w)$

Y_c	controlled element transfer function
Y_p	pilot describing function
z	log ($d\theta_w / dF_w$) or log ($1/T$)
β	sideslip angle
δ_A	spoiler/aileron deflection
ϵ	spoiler actuator valve error = R - C
θ_w	wheel angle
ζ_d	dutch roll damping ratio
ζ_ϕ	numerator damping ratio for ϕ/δ_A transfer function
ϕ	bank angle
ϕ_H	helicopter-simulator bank angle
ω	frequency of oscillation
ω_d	dutch roll frequency
ω_ϕ	numerator frequency for ϕ/δ_A transfer function

Superscript

(.)	derivative with respect to time

Abbreviations and Subscripts

ACT	actuator
DFG	diode-function-generator
HYD	hydraulic
max	maximum value of a subscripted variable
PIO	value of subscripted variable in "Pilot Induced Oscillation" situation

AIRCRAFT CONFIGURATION	SMALL STOL A/C				MEDIUM STOL A/C
	BASIC	$+C_{n_{\delta A}}$	+ DIHEDRAL	+ FIN CHANGE	BASIC
WEIGHT - LB	7000				37,000
WING AREA - FT^2	375				860
SPAN - FT	58				93
ROLL CHARACTERISTICS ζ_d	.253	.253	.196	.285	.185
ζ_φ *	.238	.210	.240	.275	.359
ω_d RAD/SEC	.150	.150	.164	.199	.894
$\omega_{\varphi}/\omega_d$ *	.818	.765	.747	.880	.850
T_R SEC	.258	.258	.252	.256	.827
T_S SEC **	-20.7	-20.7	-74.6	-17.4	343

* BASED ON THE INITIAL GRADIENT OF ROLL ACCELERATION CURVE 4 (FIGURE 9)
** NEGATIVE SIGN MEANS DIVERGENT

AIRCRAFT CHARACTERISTICS

TABLE 1

CONTROL CONFIGURATIONS	SMALL STOL AIRCRAFT			MEDIUM STOL AIRCRAFT
	MANUAL	POWERED - MANUAL	FULLY - POWERED	MANUAL
WHEEL ROTATION - DEGREES	± 75.0 →			
RADIUS - INCHES	7.0 →			
CONTROL INERTIA (I) AT WHEEL - FT LB PER RAD/$_{SEC}^2$	.078	.078	~ 0	.10
VISCOUS DAMPING (c) AT WHEEL - FT LB PER RAD/$_{SEC}$	NON-LINEAR		~ 0	4.0
STATIC FORCE AT WHEEL F_W (θ_W)	NON-LINEAR SEE FIGURE 8 →			
SPOILER CHARACTERISTICS				
ROLL ACCELERATION $\ddot{\Phi}(\theta_W)$	NON-LINEAR SEE FIGURE 9 →			
$\ddot{\Phi}$ MAX - RAD/$_{SEC}^2$	2.42	1.81	2.42	.826
ACTUATOR VALVE/WHEEL GEARING - INCHES/$_{RAD}$	—	1.36	1.36	—
MAX VALVE DISPLACEMENT (E) - INCHES	—	.0714	.0714	—
VALVE FORCE - PRELOAD (Fw_o)/GRADIENT AT THE WHEEL - LB/LB PER INCH	—	16.5/.757	—	—
AILERON CHARACTERISTICS				
ROLL ACCELERATION $\ddot{\Phi}(\theta_W)$	—	LINEAR	—	—
$\ddot{\Phi}_{MAX}$ - RAD/$_{SEC}^2$	—	0.61	—	—
RUDDER CHARACTERISTICS				
PEDAL DISPLACEMENT - INCHES	± 3.5 →			
STATIC FORCE GRADIENT AT PEDALS - LB/IN.	10 →			
ELEVATOR CHARACTERISTICS				
STICK DISPLACEMENT - INCHES	± 4 →			
STATIC FORCE GRADIENT AT STICK - LB/IN.	1.5 →			

CONTROL SYSTEM CHARACTERISTICS

TABLE 2

PILOT	HELICOPTER & HELICOPTER SIMULATOR	STOL	CONVENTIONAL PROPELLER	JET	OTHER
1	5	6000	4000	250	25
2	25	6000	9000	100	3000
3	1500	50	400	800	
4	570	30	2300	30	5

PILOT FLIGHT EXPERIENCE (HOURS)

TABLE 3